Synthesis, chemical characterization, and μ-opioid receptor activity assessment of the emerging group of nitazene new synthetic opioids

Running title: Characterization of nitazene new synthetic opioids

Marthe M. Vandeputte[1], Katleen Van Uytfanghe[1], Nathan K. Layle[2], Danielle M. St. Germaine[2], Donna M. Iula[2], Christophe P. Stove[1]

[1]Laboratory of Toxicology, Department of Bioanalysis, Faculty of Pharmaceutical Sciences, Ghent University, Ghent, Belgium

[2] Forensic Chemistry Division, Cayman Chemical, Ann Arbor, Michigan, USA

Corresponding author: Christophe P. Stove (christophe.stove@ugent.be)

Word count: 5284

Acknowledgments

We gratefully acknowledge Chiron for the gifting of etonitazene. The knowledgeable lab technicians of the Laboratory of Toxicology are acknowledged for performing part of the experiments for the analytical characterization. This work was supported by the Research Foundation-Flanders (FWO) (grant no. 3S038719 to M.V.). C.S. would like to thank the Ghent University Special Research Fund (BOF) (grant no. 01J15517).

Conflict of interest

The authors declare no conflicts of interest.

Data availability statement

The data that support the findings of this study are available from the corresponding author upon reasonable request. Some data may not be made available because of privacy or ethical restrictions.

Bullet point summary

What is already known

Nitazenes, such as isotonitazene, are increasingly misused synthetic opioids with a high harm potential.

What this study adds

Synthesis, analytical characterization, and μ-opioid receptor activity assessment of nine emerging nitazenes and three metabolites.

Clinical significance

The extensive characterization may contribute to increased awareness and detection of potentially highly dangerous nitazenes.

Abstract

Background & Purpose

Several benzimidazole opioids (commonly known as nitazenes) have recently started to emerge on the illicit market. The most frequently encountered member, the highly potent isotonitazene, has been identified in multiple fatalities since its appearance in 2019. Although recent scheduling efforts targeted isotonitazene, many other analogues remain unregulated. Being structurally unrelated to fentanyl, little is known about the harm potential of these compounds. This study describes the synthesis, analytical characterization, and μ-opioid receptor (MOR) activity of nine nitazenes and three metabolites.

Experimental Approach

Chemical characterization was performed by liquid chromatography coupled to diode array detection (LC-DAD), gas chromatography-mass spectrometry (GC-MS), and time-of-flight mass spectrometry (LC-QTOF-MS). The MOR potency and efficacy of the nitazenes was determined by means of two cell-based β-arrestin2/mini-Gi recruitment assays.

Key Results

Based on absorption spectra and retention times, HPLC-DAD allowed differentiation between most analogues. LC-QTOF-MS identified a fragment with *m/z* 100.11 for 11/12 compounds, which could serve as a basis for MS-based nitazene screening. MOR activity determination confirmed that nitazenes are generally highly active, with potencies and efficacies of several analogues exceeding that of fentanyl. Particularly relevant is the unexpected (extremely) high potency of the *N*-desethyl-isotonitazene metabolite, rivalling the potency of etonitazene and exceeding that of isotonitazene itself. Supported by its identification in fatalities, this likely has *in vivo* consequences.

Conclusion & implications

The increasing emergence of nitazenes illustrates the continuously evolving nature of the illicit drug market. Nitazenes are potent MOR agonists. As their use may pose an imminent threat to any user, intensive monitoring and increased awareness are of critical importance.

Graphical abstract

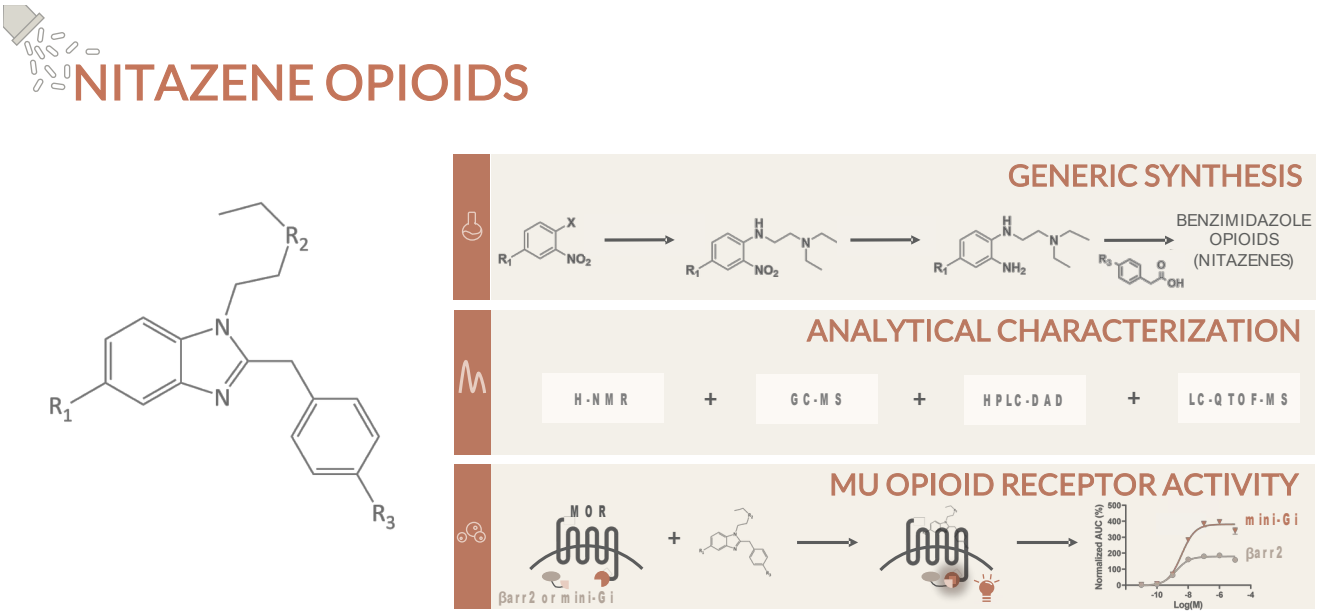

Vandeputte, et al. *Br. J. Pharmacol.*

Introduction

For several years, the presence of new synthetic opioids on the illicit drug market has been increasing (UNODC, 2020a, 2020b). Almost 80 synthetic opioids have been detected since 2009 (UNODC, 2020b). While these compounds represent a smaller share of the total portfolio of new psychoactive substances (NPS), the highly potent nature of many of these compounds poses a very high risk of poisoning (EMCDDA, 2020a). In addition, as with many NPS, the opioid market is diversifying relentlessly, with high potency opioids continuously (re-)appearing. Between 2008 and 2018, newly identified opioid NPS mainly encompassed fentanyl derivatives, which are now increasingly controlled (Bao et al., 2019). As a result, the balance recently tipped towards non-fentanyl analogues (EMCDDA, 2020a; UNODC, 2020b). In many cases, the synthesis of these newly abused synthetic opioids can be traced back to early research articles exploring their potential as novel opioid analgesics. However, due to side effects and addiction liability, most compounds were never marketed (UNODC, 2020b). Nowadays, underground chemists increasingly find their way to these original publications in search of new drugs to diversify the recreational drug market and continuously evade legislation. Recent examples include the emergence of AP-237, piperidylthiambutene, brorphine and several benzimidazole opioids, also known as nitazenes (Blanckaert et al., 2020; Cannaert et al., 2020; EMCDDA, 2020a; UNODC, 2020b; Vandeputte et al., 2020; Verougstraete et al., 2020).

Structurally unrelated to traditional opiates or fentanyl **(Fig. 1)**, the synthesis of a series of benzimidazole derivatives was first reported in the late 50s and early 60s by a Swiss company (Hunger et al., 1957, 1960a, 1960b, 1960c, 1961; Rossi et al., 1960a, 1960b). In mice, the analgesic effect of several benzimidazoles exceeded that of morphine, the potency of etonitazene, the most potent derivative, being a 1000-fold higher than that of morphine (Gross and Turrian, 1957; Hunger et al., 1960b). While several benzimidazole derivatives were patented (Hoffmann et al., 1959, 1960, 1962), further development was halted and no benzimidazole analgesics have ever been clinically approved (EMCDDA, 2020b, 2020c).

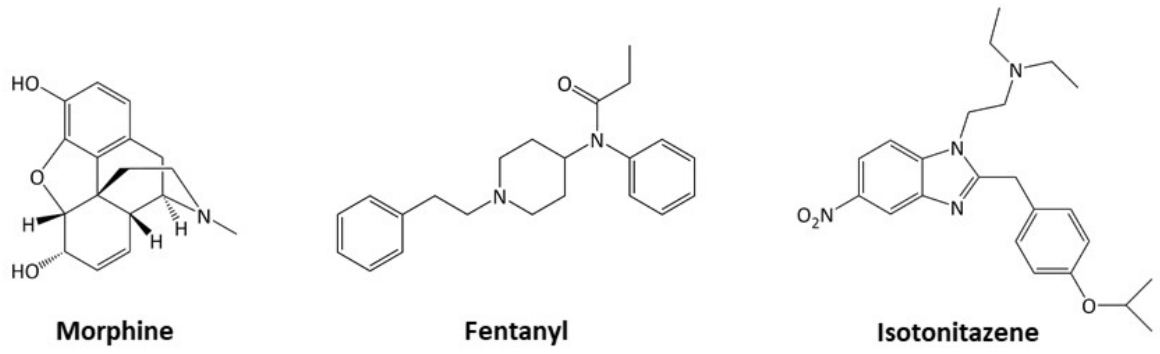

Figure 1. Structures of morphine, fentanyl, and isotonitazene. Isotonitazene, the prototypical member of the benzimidazole opioids, is structurally unrelated to traditional opiates or fentanyl.

Already in 1975, the chemist Alexander T. Shulgin warned for the potential misuse of benzimidazole opioids as heroin substitutes (Shulgin, 1975). Apart from sporadic reports on etonitazene between 1966 and 2003 (Brandenberger, 1974; Morris, 2009; Reavy, 2003; Sorokin, 1999; Sorokin et al., 1999), it wasn't until quite recently that the first benzimidazoles started to emerge on drug forums and the illicit market. March and April 2019 mark the earliest (known) appearances of isotonitazene **(Fig. 1)**, a 5-nitro-2-benzylbenzimidazole opioid, on the drug scene in Canada and Europe (EMCDDA,

2020c). Later that year, isotonitazene was identified in a powder sourced from an online NPS marketplace and was fully characterized (Blanckaert et al., 2020), generating the first report on isotonitazene since its synthesis (Hoffmann et al., 1959, 1960; Hunger et al., 1960b). Following this report, isotonitazene was formally notified to the European Monitoring Centre for Drugs and Drug Addiction (EMCDDA, 2020b). In the United States, isotonitazene was first found in biological samples in August 2019 (Krotulski and Logan, 2019; Krotulski et al., 2019, 2020a) and has since been identified in over 250 deaths (A. Krotulski, personal communication). The DEA issued a notice of intent to temporarily place isotonitazene in Schedule I in June 2020 (DEA, 2020) and this went into effect August 2020. Likewise, a ban on the compound has been initiated in Europe (European Commission, 2020). While these legislations are expected to cover isotonitazene and its isomers, esters, ethers, and corresponding salts, many other nitazenes remain unscheduled. In fact, apart from clonitazene and etonitazene, which are controlled under the United Nations Single Convention on Narcotic Drugs of 1961, none of the previously described benzimidazole opioids are currently under (international) control. Hence, the scheduling of isotonitazene can be anticipated to cause a dynamic shift towards the distribution and use of these non-scheduled analogues, as has been observed before for fentanyl analogues.

Recent chatter on drug fora indeed points at a (re)new(ed) interest in these benzimidazole opioids, and their (online) availability seems to be increasing. Metonitazene, for example, was recently found in seized material in the US (Krotulski et al., 2020b). An increasing number of desnitro-nitazenes, lacking the 5-nitro-group on the benzimidazole ring (Hunger et al., 1960a), have also started to enter the drug circuit. The first of these, etodesnitazene/etazene, was very recently seized in Poland (Siczek et al., 2020). The known high potency and overdose risk of some nitazenes (e.g. etonitazene, isotonitazene), combined with the increasing availability, poses a potentially great public health threat. In addition, their presence can be easily missed in intoxication cases, as these compounds are currently not routinely screened for and may be present at very low concentrations, requiring highly sensitive analytical instrumentation for detection (EMCDDA, 2020c; Krotulski et al., 2020a). To better substantiate our knowledge on this potentially highly dangerous class of new synthetic opioids, this report describes the synthesis, chemical characterization, and μ-opioid receptor (MOR) activity of a set of emerging nitazenes, including three metabolites of the highly potent isotonitazene **(Fig. 2)**.

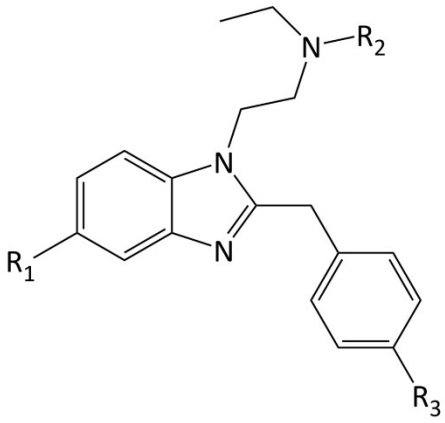

	R_1	R_2	R_3
1. Isotonitazene	$-NO_2$	$-C_2H_5$	$-OCH(CH_3)_2$
2. *N*-desethyl-isotonitazene	$-NO_2$	-H	$-OCH(CH_3)_2$
3. 4'-OH-nitazene	$-NO_2$	$-C_2H_5$	-OH
4. 5-aminoisotonitazene	$-NH_2$	$-C_2H_5$	$-OCH(CH_3)_2$
5. Metonitazene	$-NO_2$	$-C_2H_5$	$-OCH_3$
6. Etonitazene	$-NO_2$	$-C_2H_5$	$-OC_2H_5$
7. Protonitazene	$-NO_2$	$-C_2H_5$	$-OC_3H_7$
8. Clonitazene	$-NO_2$	$-C_2H_5$	-Cl
9. Flunitazene	$-NO_2$	$-C_2H_5$	-F
10. Isotodesnitazene	-H	$-C_2H_5$	$-OCH(CH_3)_2$
11. Metodesnitazene (metazene)	-H	$-C_2H_5$	$-OCH_3$
12. Etodesnitazene (etazene)	-H	$-C_2H_5$	$-OC_2H_5$

Figure 2. Generic structure of the twelve studied nitazenes. Full chemical structures are shown in **Supplementary Data S1**.

Methods

Materials

All chemical structures used in this study are depicted in **Figure 2** (generic scaffold) and in **Supplementary Data S1.** Hydromorphone was purchased as hydrochloride salt from Fagron (Nazareth, Belgium). Fentanyl was obtained as a free base from LGC Chemicals (Wesel, Germany). Morphine was purchased from Cayman Chemical Company (Ann Arbor, MI, USA). Etonitazene HCl **(6)** was procured from Chiron (Trondheim, Norway). The human embryonic kidney (HEK) 293T cells (passage 20) were kindly gifted by Prof. O. De Wever (Ghent University Hospital, Belgium). Dulbecco's Modified Eagle's Medium (DMEM; GlutaMAX™), Opti-MEM® I Reduced Serum Medium, penicillin-streptomycin (5000 U/mL) and amphotericin B (250 µg/mL) were supplied by Thermo Fisher Scientific (Pittsburg, PA, USA). Fetal bovine serum (FBS) and poly-D-lysine were purchased from Sigma Aldrich (Overijse, Belgium). The Nano-Glo® Live Cell Assay system, containing the Nano-Glo® Live Cell Substrate and Nano-Glo® LCS Dilution Buffer, was obtained from Promega (Madison, WI, USA). All chemicals used in the generic synthesis were purchased from standard reagent suppliers such as Sigma Aldrich (Milwaukee, WI) and were reagent-grade quality. All reagents used during the chromatographic analyses were at least of high-performance liquid chromatography (HPLC) grade.

Synthesis

The generic nitazene synthesis pathway, as outlined in the Results section, was based on published synthesis routes, utilizing commercially available starting materials where available (Carroll and Coleman, 1975; Renton et al., 2012). This yielded isotonitazene **(1)**, *N*-desethyl-isotonitazene HCl **(2)**, 4'-OH-nitazene **(3)**, 5-aminoisotonitazene **(4)**, metonitazene **(5)**, protonitazene HCl **(7)**, clonitazene **(8)**, flunitazene HCl **(9)**, isotodesnitazene citrate **(10)**, metodesnitazene HCl **(11)** and etodesnitazene citrate **(12)**. All final products were purified to >98% HPLC-UV purity by standard purification techniques. The structure and purity of all synthesized materials was confirmed via nuclear magnetic resonance spectroscopy (NMR) **(Supplementary Data S2)** and extensive analytical characterization, as outlined below. 1H-NMR spectra were obtained on either a Varian Unity Inova instrument (400 MHz) or a JEOL ECZ-400S (400 MHz). Samples were dissolved and recorded in DMSO-d6.

Analytical Characterization

Analytical characterization via HPLC coupled to diode array detection (HPLC-DAD), gas chromatography mass spectrometry (GC-MS) (except for **(3)**) and liquid chromatography coupled to time-of-flight mass spectrometry (LC-QTOF-MS) was done as described before (Blanckaert et al., 2020). The details of each technique are briefly summarized below.

High-performance liquid chromatography coupled to diode array detection (HPLC-DAD)

Reversed-phase separation was performed on a LaChrom HPLC system from Merck-Hitachi (Tokyo, Japan), using a Merck Purospher® Star RP-8 endcapped column (5 µm, 125 mm x 4.6 mm) fitted with a Merck Purospher® Star RP-8 endcapped guard column (5 µm, 4 mm x 4 mm). Detection was done via DAD, monitoring a wavelength from 220 – 350 nm with a slit of 1 nm, a spectral bandwidth of 1 nm and a spectral interval of 200 msec. Concentrations of the injected dilutions ranged from 8 to 40 µg/mL.

Gas chromatography mass spectrometry (GC-MS)

One µL of a 1 mg/mL solution was injected on an Agilent 7890A GC system coupled to a 5975 XL mass-selective detector operated by MSD Chemstation software, as described in (Blanckaert et al., 2020). The mass spectrometer operated in SCAN-mode, scanning the range of 50 – 700 Da. For 4'-OH-nitazene **(3)**, one µL of a 1 mg/mL solution was injected on an Agilent 8890 GC system coupled to a 5977 mass-selective detector operated by OpenLabs CDS software. Injections with a split ratio of 15:1 were performed automatically at an injection temperature of 300°C, with helium as the carrier gas at a constant flow rate of 2 mL/min. A 30 m x 0.32 mm i.d. x 0.5 µm Restek Rtx-5MS column was used. The temperature program started at 50°C for 1 min, was ramped at 30°C/min to 300°C, which was held for 16 more minutes. The transfer line temperature and ion source temperature were set at 300 and 280°C respectively. MS quadrupole temperature was set at 150 °C and an ionization energy of 70 eV was used. The mass spectrometer operated in SCAN-mode, scanning the range of 40 – 650 Da.

Liquid chromatography coupled to time-of-flight mass spectrometry (LC-QTOF-MS)

Using a 1 µg/mL solution, spectra were recorded after infusion or after chromatographic separation. The latter was accomplished with an Agilent 1290 Infinity LC system and a Phenomenex Kinetex C18-column (2.6 µm, 3 x 50 mm), maintained at 30°C. The high-resolution mass spectrometry system was a 5600+ QTOF from Sciex, with an electrospray ionization (ESI) source and Analyst TF 1.7.1 software, from the same provider. Settings for QTOF-MS were the same as published before (Blanckaert et al., 2020). The LC-QTOF-MS settings resulted in TOF-MS full scan spectra combined with data dependent acquisition of product ion spectra (both scanning from 5 to 450 Da).

Determination of *in vitro* biological activity at the µ-opioid receptor (MOR)

Cell culture

HEK 293T cells stably expressing either the MOR-βarr2-GRK2 or MOR-mini-Gi system (see below) were routinely maintained in DMEM (GlutaMAX™) supplemented with 10% heat-inactivated FBS, 100 IU/mL penicillin, 100 mg/L streptomycin and 0.25 mg/L amphotericin B. The cells were cultured at 37°C in a humidified atmosphere containing 5% CO_2. The stability of the cell lines was routinely monitored via flow cytometric analysis of co-expressed markers (Vasudevan et al., 2020).

NanoBiT MOR-β-arrestin2/mini-Gi recruitment bio-assay

Two stable cell-based reporter assays were used to assess the *in vitro* biological MOR activity of twelve different nitazenes, fentanyl, morphine and hydromorphone. The development of the employed assays has been described before (Cannaert et al., 2018a, 2019a; Vasudevan et al., 2020). In short, activation of human MOR, fused to one part of a split nanoluciferase (NanoLuc® Binary Technology, Promega), results in the recruitment of either β-arrestin2 (βarr2) (in the presence of co-expressed G protein-coupled receptor kinase 2, GRK2) or mini-Gi (GTPase domain of the Gαi subunit), fused to the complementing part of the split nanoluciferase. The resulting functional complementation of the nanoluciferase restores its enzymatic activity, which, upon addition of the substrate furimazine, will yield a measurable bioluminescent signal.

Cells expressing either MOR-βarr2-GRK2 (for simplicity, further referred to as MOR-βarr2) or MOR-mini-Gi were seeded on poly-D-lysine coated 96-well plates (5 x 10^4 cells/well) one day prior to the experiments. Following overnight incubation, the cells were washed twice with Opti-MEM® I Reduced Serum Medium before adding 90 µL OptiMEM®. Nano-Glo® Live Cell reagent was then

prepared by 20-fold dilution of Nano-Glo® Live Cell Substrate with Nano-Glo® LCS Dilution Buffer, and 25 µL was added to each well. The plate was subsequently placed into a TriStar² LB 942 multimode microplate reader (Berthold Technologies GmbH & Co., Bad Wildbad, Germany) and luminescence was continuously monitored until stabilization of the signal (10-15 minutes). Next, 20 µL of a 6.75-fold concentrated stock solution of each test compound (in Opti-MEM®/MeOH or Opti-MEM®/ACN) was added per well and luminescence was monitored for 2 hours. All compounds were tested in both assays in concentrations ranging between 1 pM and 100 µM, with appropriate solvent controls included in each experiment. Each compound was evaluated in five independent experiments (n=5), with duplicates run for each concentration within an experiment to ensure the reliability of single values.

Data and statistical analysis

The data and statistical analysis comply with the recommendations on experimental design and analysis in pharmacology (Curtis et al., 2018). Absolute time-luminescence profiles obtained during the two-hour read-out were corrected for inter-well variability and used for calculation of the area under the curve (AUC), as previously detailed by Pottie *et al.* (Pottie et al., 2020a). Solvent controls were performed by subtraction of the mean AUC of the corresponding blank. Concentration-response curves were subsequently generated via GraphPad Prism 8 software (San Diego, CA, USA) via three-parametric nonlinear regression, which implies a fixed Hill slope of 1. The use of this model is required for the implementation of the ligand bias calculation described below (Ehlert, 2008; Rajagopal et al., 2011). To facilitate interpretation and comparison between different studies, the data were normalized to the maximum response of hydromorphone (arbitrarily set at 100%) for each experiment. Hydromorphone was selected as a reference agonist for normalization based on previous experience (Blanckaert et al., 2020; Cannaert et al., 2020; Vandeputte et al., 2020; Vasudevan et al., 2020; Verougstraete et al., 2020). It was defined *a priori* that AUC values from the highest concentration(s) were excluded in case of a reduction of 20% or more compared to the AUC of the next dilution. As previously hypothesized for different receptor systems (Pottie et al., 2020b; Vandeputte et al., 2020), high concentrations may potentially lead to cell toxicity or solubility issues, with a rapid drop of the signal resulting in a lower AUC. Inclusion of such data points could inadvertently skew the obtained concentration-response graph. Using the standard Grubbs' test, the complete dataset (2080 data points) was screened for outliers, resulting in a total of 16 outliers (0.77%) that were subsequently omitted from the data set. All duplicate data points were considered separately in the Grubb's test. This means that data points were only excluded if a single value (out of e.g. n = 5 x 2) was considered an outlier in the Grubbs' test, as in this case the reliability of this single value could not be ensured. For each compound, the normalized data from five separate experiments were then combined to obtain final EC_{50} and E_{max} values, which are measures of respectively potency and efficacy (the latter relative to hydromorphone).

Pathway bias was calculated as previously described (Pottie et al., 2020b; Rajagopal et al., 2011), with hydromorphone employed as reference agonist that is considered unbiased (Vasudevan et al., 2020). First, the intrinsic relative activity (RA_i) was calculated for each compound in both bioassays (Equation 1; i = test compound and HM = unbiased reference agonist, hydromorphone) (Ehlert et al., 1999).

$$RA_{i,\,reference\,agonist}^{pathway} = \frac{\frac{E_{max,i}}{EC_{50,i}}}{\frac{E_{max,HM}}{EC_{50,HM}}} = \frac{EC_{50,HM}\,x\,E_{max,i}}{E_{max,HM}\,x\,EC_{50,i}}$$

The obtained RA_i values per pathway were then combined into a bias factor (β_i) for each individual compound according to Equation 2 (Ehlert, 2008; Rajagopal et al., 2011).

$$\beta_i = \log\left(\frac{RA_{i,HM}^{\beta arr2}}{RA_{i,HM}^{mini-Gi}}¿\right)¿$$

Compared to the reference hydromorphone (β = 0, as it is considered unbiased), compounds with a positive value for β tend to favor βarr2 recruitment, whereas a bias factor below zero indicates a certain extent of bias towards mini-Gi recruitment. The bias factor for each compound was calculated from five independent experiments, each performed in duplicate. Statistical analysis was carried out in GraphPad Prism 8 by non-parametric one-way ANOVA (Kruskal-Wallis), followed by a post hoc Dunn's test. Differences were considered statistically significant when $p < 0.05$.

Results

Synthesis

Figure 3 shows a scheme depicting the generic synthesis route for the nitazenes reported here **(1-12, Fig. 2)**. For analogues **(1)**, **(3)**, and **(5-12)**, an appropriately substituted nitrobenzene **(I)** was reacted with *N*,*N*-diethylethylenediamine to afford synthetic intermediate **II**. The nitro group that is *ortho* to the amino group of intermediate **II** was then selectively reduced using aqueous ammonium sulfide (or a suitable equivalent) in refluxing ethanol to afford **III**. Condensation of **III** with an appropriately substituted phenylacetic acid derivative (such as in the presence of *N*-ethoxycarbonyl-2-ethoxy-1,2-dihydroquinoline) afforded the desired benzimidazoles as free bases. Hydrochloric or citric acid was used to convert some of the resulting benzimidazoles into their corresponding salt forms.

N-desethyl-isotonitazene **(2)** was prepared in a similar fashion as described above, except that *N*-Boc-*N*-ethylethylenediamine was used in place of *N*,*N*-diethylethylenediamine in the first step of the synthesis. The Boc protecting group was carried through the subsequent steps and the final product was then treated with trifluoroacetic acid to remove the protecting group. Lastly, treatment with hydrochloric acid afforded compound **(2)** as the corresponding HCl salt. 5-aminoisotonitazene **(4)** was prepared by treating isotonitazene **(1)** under standard hydrogenation conditions to reduce the nitro group to the corresponding primary amine.

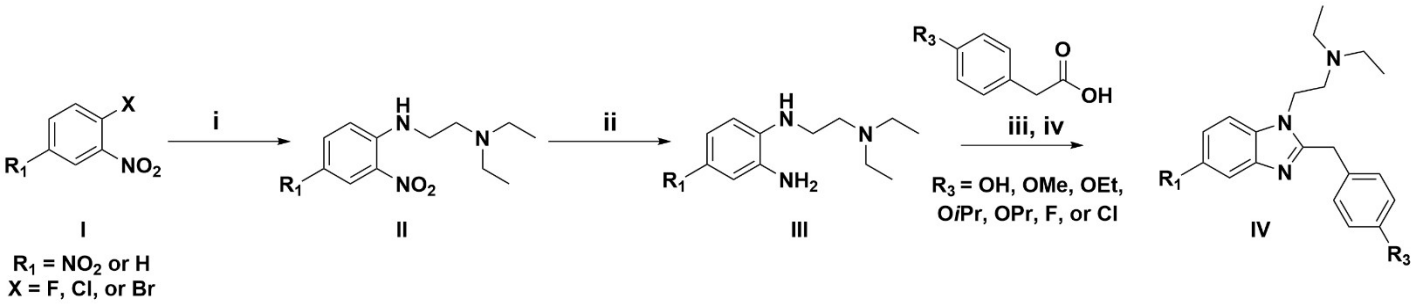

Figure 3. General scheme depicting the synthesis of the different nitazenes included in this study **(1-12)** (Carroll and Coleman, 1975; Renton et al., 2012). Reagents and conditions: **(i)** *N*,*N*-diethylethylenediamine, EtOH, reflux; **(ii)** $(NH_4)_2S$,

EtOH, reflux; **(iii)** *N*-ethoxycarbonyl-2-ethoxy-1,2-dihydroquinoline, CH_2Cl_2; **(iv)** HCl for **(7), (9)** and **(11)** or citric acid for **(10)** and **(12)**.

Analytical characterization

A summary of the key findings of the analytical characterization can be found in **Table 1**. **Figure 4** provides a graphical representation of the fragments found by QTOF-MS. **Supplementary Data S3** includes a more detailed representation of the fragmentation pathway, based on A. Weissberg et al. (Weissberg et al., 2016). **Supplementary Data S4 – S6** contain all relevant individual chromatograms and spectra. The obtained spectra match those that were previously reported by our group for isotonitazene (Blanckaert et al., 2020) and by other research groups or manufacturers (Cayman Chemical Company, 2020; Krotulski et al., 2020a; Shamai Yamin et al., 2018; Weissberg et al., 2016).

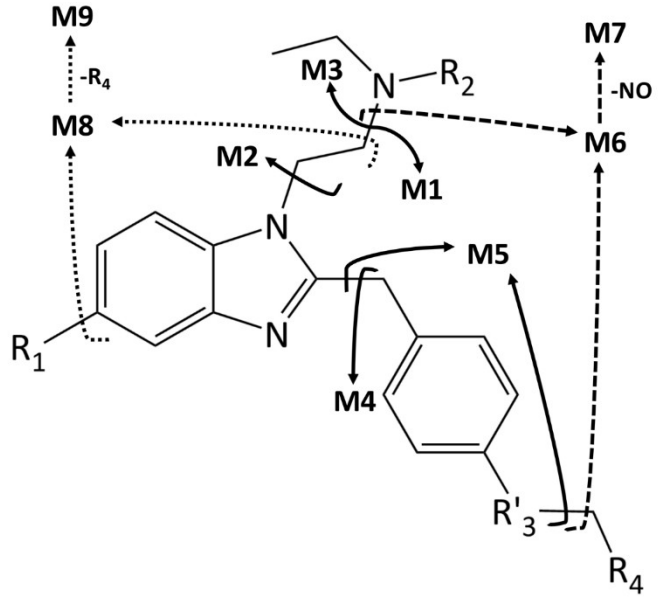

Fragment	Fragment found for
M1	3, 5, 6, 7, 8, 9, 11, 12
M2	1, 2, 3, 4, 5, 6, 7, 8, 9, 10, 11, 12
M3	1, 3, 4, 5, 6, 7, 8, 9, 10, 11, 12
M4	1, 3, 4, 5, 6, 7, 8, 9, 10, 11, 12
M5	1, 2, 4, 6, 7, 10, 12
M6	1, 10
M7	4
M8	3, 5, 6, 7, 8, 9, 11
M9	7

Figure 4. Graphical representation of the different fragments found by QTOF-MS. Different styles of arrows were used to allow easy identification of fragmentations that result in a given fragment.

Bio-assay data

In vitro μ-opioid receptor activity

The MOR activity of all twelve nitazenes was evaluated using two recruitment assays (MOR-βarr2 and MOR-mini-Gi), generating receptor activation profiles as shown in **Figure 5. Supplementary Data S7** provides an overlay of the MOR-βarr2 and MOR-mini-Gi recruitment profiles per compound. All data were normalized to the maximum response of hydromorphone. Fentanyl and morphine are included for comparison and to facilitate interpretation of the data. **Table 2** shows the derived potency (EC_{50}) and efficacy (E_{max}, relative to hydromorphone) values.

In terms of potency, *N*-desethyl-isotonitazene **(2)** and etonitazene **(6)** showed the lowest EC_{50} values (i.e., the highest potencies) in both assays. These compounds were also the most efficacious in terms of both βarr2 and mini-Gi recruitment. Metodesnitazene **(11)** was the least potent compound of this panel in both bio-assays. Together with 4'-OH-nitazene **(3)**, it was also the least efficacious. Except for *N*-desethyl-isotonitazene **(2)**, the evaluated metabolites **(3, 4)** were less active than their parent

compound isotonitazene **(1)**. As both the EC_{50} and E_{max} values were consistently higher in the mini-Gi assay than in the βarr2 assay, the former yielded overall lower potency and higher efficacy scores.

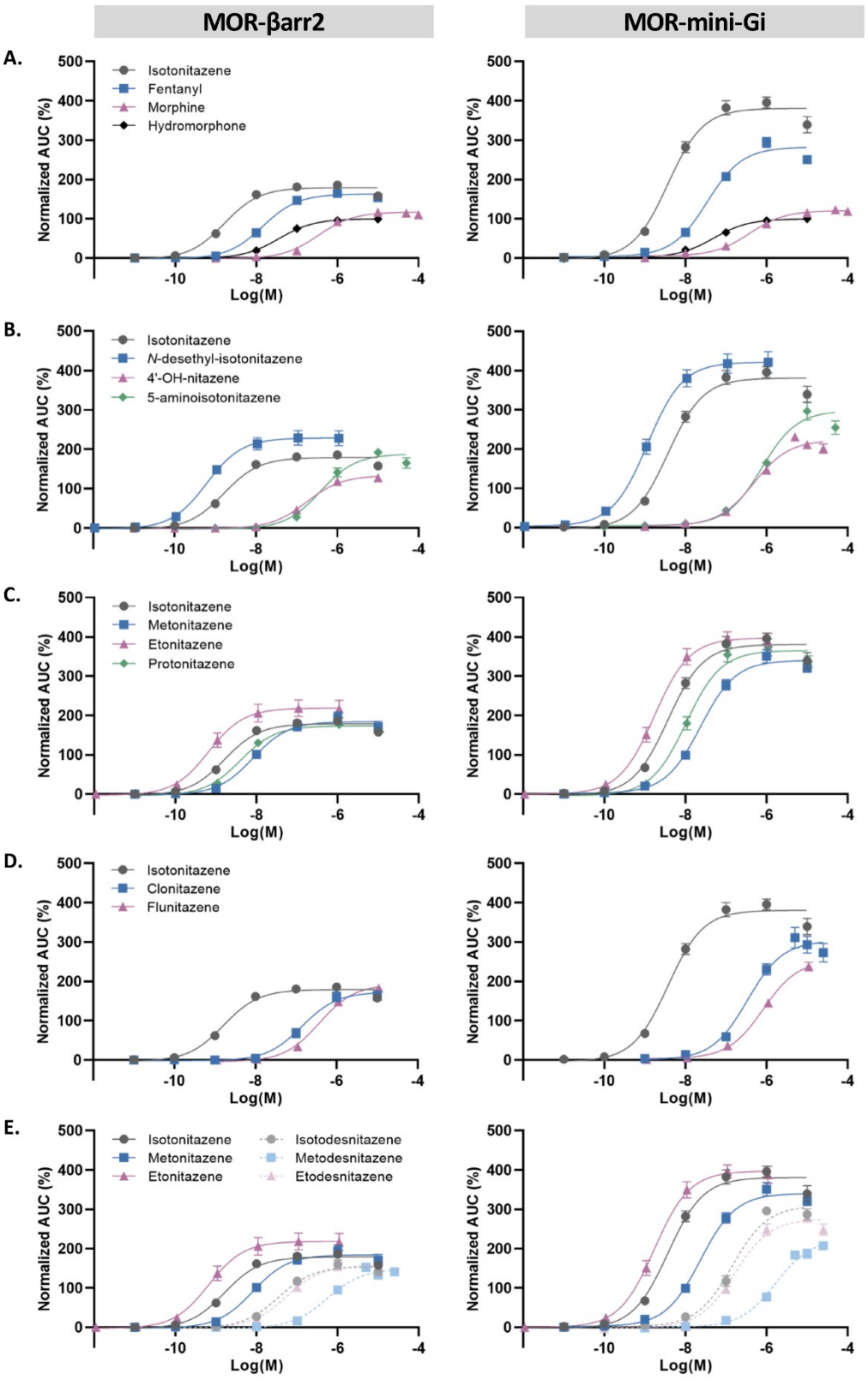

Figure 5. Activation profiles (*n*=5) obtained for isotonitazene and **(A)** fentanyl, morphine and hydromorphone; **(B)** the metabolites *N*-desethyl-isotonitazene, 4'-OH-nitazene and 5-aminoisotonitazene; **(C)** metonitazene, etonitazene and protonitazene; **(D)** clonitazene and flunitazene; and **(E)** the desnitro-nitazenes isotodesnitazene, metodesnitazene, etodesnitazene. The left and right panels present data from the μ-opioid receptor (MOR) β-arrestin 2 and mini-Gi

recruitment assays, respectively. Data are presented as mean receptor activation ± standard error of the mean (SEM) and are normalized to the maximum response of hydromorphone. Sixteen outliers (0.77%), as identified by the Grubbs' test, were excluded from the data set.

Assessment of biased agonism at the μ-opioid receptor

The employed bio-assays are highly similar, only differing in the nature of the recruited transducer molecule (βarr2 *vs.* mini-Gi). This lends the current set-up particularly suitable to assess biased agonism at MOR. In **Figure 6**, the bias factors (β, see Methods) for all compounds are plotted in a quantitative MOR bias plot. Compared to hydromorphone, the unbiased reference agonist (β = 0), none of the compounds evaluated in this study showed statistically significant biased agonism at MOR.

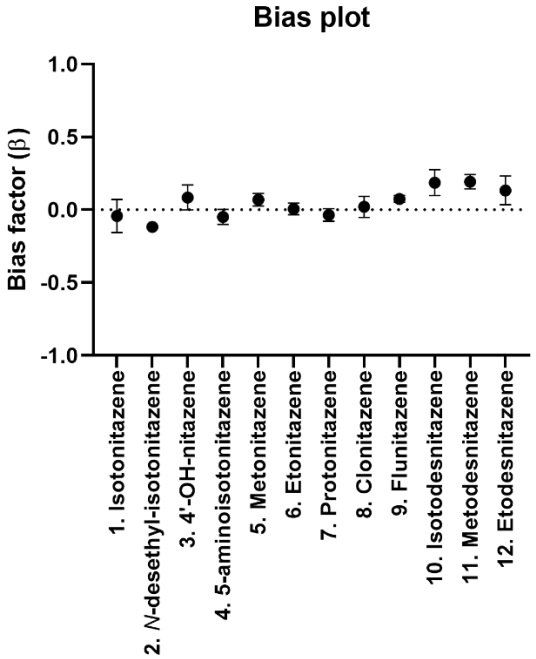

Figure 6. Quantitative μ-opioid receptor bias plot. Bias factors (β) ± SEM are plotted for all tested compounds, calculated from five independent experiments (*n*=5). Hydromorphone was used as unbiased reference agonist (β=0, not shown). Positive or negative bias factors imply a preference towards βarr2 or mini-Gi recruitment, respectively. None of the evaluated compounds showed statistically significant biased agonism at MOR, as compared to hydromorphone.

Discussion & Conclusions

This study reports the synthesis, analytical characterization, and *in vitro* MOR activity assessment of 12 benzimidazoles (commonly referred to as nitazenes), a class of opioids increasingly appearing on the illicit drug market. Apart from a series of research articles exploring their potential as analgesics in the 1950s-1960s, alarmingly little is known about these compounds and the risks associated with their use. This report therefore aims to address current knowledge gaps and increase public awareness of these newly emerging opioids.

Benzimidazole opioids can be synthesized via different pathways readily described in literature (Carroll and Coleman, 1975; Hoffmann et al., 1959, 1960; Hunger et al., 1957, 1960a, 1960b; Kim et al., 2011; Renton et al., 2012). While it is not clear which route(s) are used for their illicit manufacture, several methods are simple and cost-efficient, not requiring regulated precursors (Zagorski et al., 2020). For this report, we applied a relatively simple generic route (Carroll and Coleman, 1975; Renton et al., 2012). The nitazenes synthesized here were extensively characterized analytically via 1H-NMR, HPLC-DAD, GC-MS, and LC-QTOF-MS. Although even HPLC-DAD could differentiate most analogues based on absorption spectra and retention times, MS-based techniques allowed unequivocal identification and are required for identification in biological matrices. Using chromatography coupled to MS, even isomers could be distinguished based on differences in retention times and/or specific fragments. Most analogues have very similar fragment spectra, apart from *N*-desethyl-isotonitazene, which is to be expected based on its structure. Given that, for all other analogues, the fragment with *m/z* 100.11 is the most abundant in QTOF-MS, this fragment may be selected as a trigger for a precursor ion scan. Hence, this fragment may serve as a diagnostic marker for a specific (high-resolution) MS-based nitazene screening method. Developing highly specific targeted liquid chromatography tandem mass spectrometry (LC-MS/MS) methods should also be possible given that, for most compounds, a combination of a specific parent/fragment mass can be made.

Using two different *in vitro* MOR activation assays, we found that all tested nitazenes were active at MOR, the primary molecular target for clinically applied and abused opioids (Charbogne et al., 2014). In fact, in both assays, efficacies up to 1.4-fold that of fentanyl were found, potentially indicating that even stronger opioid effects may be reached with most nitazenes, as compared to fentanyl. When considering potencies in both bio-assays *versus* that of fentanyl, the evaluated nitazenes could be classified into roughly four categories: those with a potency around (A) 20 times higher **(2, 6)**; (B) 2-10 times higher **(1, 5, 7)**; (C) 2-10 times lower **(8, 10, 12)**; and (D) 12-50 times lower **(3, 4, 9, 11)** than that of fentanyl. In line with observations by Krotulski *et al.* (2020b), who noted lower isotonitazene concentrations in biological samples from fatalities than those typically found for fentanyl, it can be expected that for nitazenes from groups (A) and (B), lower doses may be sufficient to yield significant opioid effects. This stresses the high harm potential of even small quantities of material and emphasizes the need for highly sensitive detection methods – whether analytical or activity-based (Cannaert et al., 2018a, 2018b, 2019b, 2019a, 2019c; Verougstraete et al., 2020). In a recent report from Poland, undiluted etodesnitazene was identified in a powder. As also stated by the authors, the fact that a large amount (25.0 g) of highly pure powder was found, poses a particular threat (Siczek et al., 2020). While the exact dosage regimens for most opioids remain hard to predict (depending on e.g. existing tolerance, desired effects), the high potency of etodesnitazene **(12)** found in this study, further underscores this warning. Similarly, undiluted isotonitazene **(1)** was recently identified in a

powder. Considering its high potency and efficacy, this was also considered a distinct risk to users (Blanckaert et al., 2020).

Isotonitazene was the first of the nitazenes that recently (re-)appeared on the drug market, where it has since been involved in multiple fatalities (Blanckaert et al., 2020; EMCDDA, 2020b; Krotulski and Logan, 2019; Krotulski et al., 2020a). The exact role of isotonitazene in these deaths, however, often remains speculative (EMCDDA, 2020c). Additionally, based on the results presented here, the presence of (one or more) active metabolite(s) may also contribute to the observed toxicity. We found that all three evaluated isotonitazene metabolites **(2-4)** still caused receptor activation. Of particular interest is the unexpected (extremely) high activity of the *N*-desethyl/nor-metabolite **(2)**. With an EC_{50} rivalling that of etonitazene – previously the most active benzimidazole opioid known – the potency of this metabolite exceeds that of isotonitazene itself. This likely has *in vivo* consequences, as also implied by its identification in fatalities in the US and the UK (EMCDDA, 2020c; Krotulski et al., 2020a). Reduction of the 5-nitro group of isotonitazene results in the 5-amino-metabolite **(4)**, a transformation that is accompanied with an activity decrease. As also hypothesized by Krotulski and colleagues (2020b), the 4'-OH-metabolite **(3)** is expected to be a common metabolite for several of the herein evaluated benzimidazoles. However, with a 100-fold lower potency than isotonitazene, it is doubtful that this metabolite will significantly contribute to the overall *in vivo* effect of most analogues (EMCDDA, 2020c). Considering 4'-OH-nitazene as a potential substance of abuse itself, higher doses (as compared to the main compounds) will be needed to obtain significant opioid effects. This matches the data from mouse studies, where similar analgesic effects were observed with 4'-OH-nitazene as with morphine (Hunger et al., 1960b). With the caveat that it remains difficult to directly compare *in vivo* and *in vitro* results, this is roughly in line with the data presented here.

Our data show that a number of different variations to the general (2-benzyl-)benzimidazole structure drastically impact the activity at MOR. Given the increasing scheduling efforts targeting isotonitazene, a gradual shift towards the use of such analogues can be expected (Siczek et al., 2020). What follows is a discussion of the structure-activity relationships of benzimidazoles differing from isotonitazene in the length of the alkoxy-chain **(5-7)**, the type of *para*-benzyl substituent **(8, 9)** and the presence of a 5-nitro group **(10-12)**. Our *in vitro* results are discussed and compared with the findings of *in vivo* (mouse) studies. Besides possible species differences, it should be emphasized that the eventual *in vivo* effect in humans is the result of a complex interplay of multiple factors (including bioavailability, metabolic stability, blood-brain-barrier permeability, tolerance, …), complicating a direct comparison with the obtained *in vitro* activity data. Nevertheless, the comparison with the well-known compounds morphine and fentanyl, as well as the implication of isotonitazene in fatalities, provides a framework that allows an estimation of the potential harmfulness of these compounds.

Changing the length of the *para*-alkoxy side chain from isopropoxy **(1)** to propoxy, ethoxy, or methoxy, respectively yields protonitazene **(7)**, etonitazene **(6)**, and metonitazene **(5)**. Of these, the *para*-ethoxy substituent in etonitazene **(6)** yields the highest potency in both assays, followed by -isopropoxy, -propoxy, and -methoxy. Interestingly, this ranking matches that found in animal studies, where these compounds were compared with morphine (Gross and Turrian, 1957; Hunger et al., 1960b). In terms of efficacy, the E_{max} values of isoto-, meto- and protonitazene were roughly similar, while etonitazene remained the most efficacious compound. Overall, these results indicate that

either a relatively short (ethoxy) or more compact (isopropoxy) alkoxy-tail is optimal for MOR activation. As also indicated by Hunger and colleagues (1960a, 1960b), shortening or further lengthening of the alkoxy-chain is not expected to increase MOR activity.

Halogenated compounds, in which the *para*-alkoxy tail is replaced by a chlorine or fluorine halogen, are represented by clonitazene **(8)** and flunitazene **(9)**, respectively. In line with *in vivo* findings (Hunger et al., 1957, 1960b), we found that halogenation results in a drastically decreased potency, relative to isotonitazene. In a mouse tail-flick assay, clonitazene was reported to be three times more potent than morphine, while the analgesic potency of flunitazene was comparable to that of morphine (Hunger et al., 1960b). This corresponds remarkably well with the *in vitro* MOR-βarr2 data reported here, where $EC_{50,morphine} \approx EC_{50,flunitazene} \approx 2.4 \times EC_{50,clonitazene}$.

Desnitro-nitazenes **(10-12)** represent the third class of benzimidazole analogues evaluated here. Animal studies previously showed that the activity of metodesnitazene approaches that of morphine. Upon further lengthening of the alkoxy-chain to etodesnitazene, the effect of morphine was exceeded about 70 times (Hunger et al., 1960a). This trend is mirrored in our *in vitro* MOR-βarr2 results, where the potency of etodesnitazene largely exceeds that of metodesnitazene and morphine. In the MOR-mini-Gi assay, metodesnitazene was up to 4 times less potent than morphine, whereas etodesnitazene remained about twice as potent. The efficacies of **(10-12)** were largely similar in the MOR-βarr2 assay, while differing slightly more in the mini-Gi assay. All three evaluated desnitro-nitazenes were generally less active than their 5-nitro counterparts **(1, 5, 6)**. Together with *in vivo* data, these results indicate an important role for the 5-nitro group in the activity at MOR. This is supported by the results for 5-aminoisotonitazene **(4)**, where reduction of the 5-nitro group led to a >200-fold reduced potency, when compared to isotonitazene.

In addition to investigating structure-activity relationships, the complementary nature of the employed bio-assays also allowed characterization of the nitazenes in terms of potential biased agonism (Wootten et al., 2018), a recently debated subject in the field of MOR research (Gillis et al., 2020). This work adds valuable insights to that discussion, as none of the evaluated nitazenes were significantly biased. This is in line with recent studies on fentanyl analogues (Vasudevan et al., 2020) and non-fentanyl opioids (Vandeputte et al., 2020), in which, similarly, no bias could be detected with the assays deployed here.

As the presence of non-fentanyl opioids on the drug market continues to rise, it will become increasingly important to rapidly identify and characterize new compounds as they emerge. Nitazenes are among the newest to appear and, given their high opioid activity, they pose an alarming threat to users. The extensive chemical and pharmacological characterization performed here may contribute to increased awareness and detection of this potentially highly dangerous class of new synthetic opioids.

References

Bao, Y., Meng, S., Shi, J., and Lu, L. (2019). Control of fentanyl-related substances in China. The Lancet Psychiatry *6*, e15.

Blanckaert, P., Cannaert, A., Van Uytfanghe, K., Hulpia, F., Deconinck, E., Van Calenbergh, S., and Stove, C.P. (2020). Report on a novel emerging class of highly potent benzimidazole NPS opioids: Chemical and in vitro functional characterization of isotonitazene. Drug Testing and Analysis *12*, 422–430.

Brandenberger, H. (1974). Die Rolle des Massenspektrometers im toxikologisch-chemischen Laboratorium. Deutsche Lebensmittel-Rundschau *70(1)*, 31–39.

Cannaert, A., Vasudevan, L., Friscia, M., Mohr, A.L.A., Wille, S.M.R., and Stove, C.P. (2018a). Activity-Based Concept to Screen Biological Matrices for Opiates and (Synthetic) Opioids. Clinical Chemistry *64*, 1221–1229.

Cannaert, A., Storme, J., Hess, C., Auwärter, V., Wille, S.M.R., and Stove, C.P. (2018b). Activity-Based Detection of Cannabinoids in Serum and Plasma Samples. Clinical Chemistry *64*, 918–926.

Cannaert, A., Deventer, M., Fogarty, M., Mohr, A.L.A., and Stove, C.P. (2019a). Hide and Seek: Overcoming the Masking Effect of Opioid Antagonists in Activity-Based Screening Tests. Clinical Chemistry *65*, 1604–1605.

Cannaert, A., Vandeputte, M.M., Wille, S.M.R., and Stove, C.P. (2019b). Activity-based reporter assays for the screening of abused substances in biological matrices. Critical Reviews in Toxicology *49*, 95–109.

Cannaert, A., Vandeputte, M.M., Hudson, S., Wood, D.M., Dargan, P.I., and Stove, C.P. (2019c). Validation of Activity-Based Screening for Synthetic Cannabinoid Receptor Agonists in a Large Set of Serum Samples. Clinical Chemistry *65*, 347–349.

Cannaert, A., Hulpia, F., Risseeuw, M., Van Uytfanghe, K., Deconinck, E., Van Calenbergh, S., Blanckaert, P., and Stove, C.P. (2020). Report on a new opioid NPS: chemical and in vitro functional characterization of a structural isomer of the MT-45 derivative diphenpipenol. Journal of Analytical Toxicology bkaa066.

Carroll, F.I., and Coleman, M.C. (1975). Etonitazene. Improved synthesis. Journal of Medicinal Chemistry *18*, 318–320.

Cayman Chemical Company (2020). Nitazenes. Retrieved from https://www.caymanchem.com/search?q=nitazene

Charbogne, P., Kieffer, B.L., and Befort, K. (2014). 15 years of genetic approaches in vivo for addiction research: Opioid receptor and peptide gene knockout in mouse models of drug abuse. Neuropharmacology *76*, 204–217.

Curtis, M.J., Alexander, S., Cirino, G., Docherty, J.R., George, C.H., Giembycz, M.A., Hoyer, D., Insel, P.A., Izzo, A.A., Ji, Y., et al. (2018). Experimental design and analysis and their reporting II: updated and simplified guidance for authors and peer reviewers: Editorial. British Journal of Pharmacology *175*, 987–993.

DEA (2020). 21 CFR Part 1308. Schedules of Controlled Substances: Temporary Placement of Isotonitazene in Schedule I. Retrieved from

https://www.deadiversion.usdoj.gov/fed_regs/rules/2020/fr0618.htm

Ehlert, F.J. (2008). On the analysis of ligand-directed signaling at G protein-coupled receptors. Naunyn-Schmiedeberg's Archives of Pharmacology *377*, 549–577.

Ehlert, F.J., Griffin, M.T., Sawyer, G.W., and Bailon, R. (1999). A simple method for estimation of agonist activity at receptor subtypes: comparison of native and cloned M3 muscarinic receptors in guinea pig ileum and transfected cells. The Journal of Pharmacology and Experimental Therapeutics *289*, 981–992.

EMCDDA (2020a). European drug report 2020: trends and developments. (Luxembourg: Publications Office of the European Union).

EMCDDA (2020b). EMCDDA initial report on the new psychoactive substance N,N-diethyl-2,4-(1-methylethoxy)phenylmethyl-5-nitro-1H-benzimidazole-1-ethanamine (isotonitazene). (Luxembourg: Publications Office of the European Union).

EMCDDA (2020c). EMCDDA technical report on the new psychoactive substance N,N-diethyl-2-((5-(1-methylethoxy)phenyl)methyl)-5-nitro-1H-benzimidazole-1-ethanamine (isotonitazene) (Lisbon: EMCDDA).

European Commission (2020). Fight against drugs: Commission initiates ban on new harmful psychoactive substance isotonitazene. Retrieved from https://ec.europa.eu/commission/presscorner/detail/en/mex_20_1552

Gillis, A., Kliewer, A., Kelly, E., Henderson, G., Christie, M.J., Schulz, S., and Canals, M. (2020). Critical Assessment of G Protein-Biased Agonism at the μ-Opioid Receptor. Trends in Pharmacological Sciences S0165614720302157.

Gross, F., and Turrian, H. (1957). Über Benzimidazolderivate mit starker analgetischer Wirkung. Experientia *13*, 401–403.

Hoffmann, K., Hunger, A., Kebrle, J., and Rossi, A. (1959). Verfahren zur Herstellung analgetisch wirksamer Benzimidazole (DE Patent 1057123B).

Hoffmann, K., Hunger, A., and Rossi, A. (1960). Benzimidazoles (US Patent 2935514A).

Hoffmann, K., Hunger, A., Kebrle, J., and Rossi, A. (1962). Verfahren zur Herstellung neuer Benzimidazole (CH Patent 362080A).

Hunger, A., Kebrle, J., Rossi, A., and Hoffmann, K. (1957). Synthese basisch substituierter, analgetisch wirksamer Benzimidazol-Derivate. Experientia *13*, 400–401.

Hunger, A., Kebrle, J., Rossi, A., and Hoffmann, K. (1960a). Benzimidazol-Derivate und verwandte Heterocyclen II. Synthese von 1-Aminoalkyl-2-benzyl-benzimidazolen. Helvetica Chimica Acta *43*, 800–809.

Hunger, A., Kebrle, J., Rossi, A., and Hoffmann, K. (1960b). Benzimidazol-Derivate und verwandte Heterocyclen III. Synthese von 1-Aminoalkyl-2-nenzyl-nitro-benzimidazolen. Helvetica Chimica Acta *43*, 1032–1046.

Hunger, A., Kebrle, J., Rossi, A., and Hoffmann, K. (1960c). Benzimidazol-Derivate und verwandte Heterocyclen VI. Synthese von Phenyl-[1-aminoalkyl-benzimidazolyl-(2)]-essigsäure-estern und -amiden. Helvetica Chimica Acta *43*, 1727–1733.

Hunger, A., Kebrle, J., Rossi, A., and Hoffmann, K. (1961). Benzimidazol-Derivate und verwandte Heterocyclen VII. Synthese neuer 2-Amino-benzimidazole. Helvetica Chimica Acta *44*, 1273–1282.

Kim, Y., Kumar, M.R., Park, N., Heo, Y., and Lee, S. (2011). Copper-Catalyzed, One-Pot, Three-Component Synthesis of Benzimidazoles by Condensation and C–N Bond Formation. The Journal of Organic Chemistry *76*, 9577–9583.

Krotulski, A.J., and Logan, B.K. (2019). Isotonitazene. Retrieved from https://www.npsdiscovery.org/wp-content/uploads/2019/11/Isotonitazene_112119_ToxicologyAnalyticalReport.pdf

Krotulski, A.J., Papsun, D.M., Fogarty, M.F., Nelson, L., and Logan, B.K. (2019). Potent synthetic opioid - isotonitazene - recently identified in the Midwestern United States. Retrieved from https://www.npsdiscovery.org/wp-content/uploads/2019/11/Public-Alert_Isotonitazene_NPS-Discovery_111919-1.pdf

Krotulski, A.J., Papsun, D.M., Kacinko, S.L., and Logan, B.K. (2020a). Isotonitazene Quantitation and Metabolite Discovery in Authentic Forensic Casework. Journal of Analytical Toxicology *44*, 521–530.

Krotulski, A.J., Shuda, S.A., Fogarty, M.F., Decker, S.E., and Logan, B.K. (2020b). Metonitazene. Retrieved from https://www.npsdiscovery.org/wp-content/uploads/2020/07/Metonitazene_073020_NMSLabs_Report.pdf?mc_cid=c244538976&mc_eid=0872426f82

Morris, H. (2009). Synthetic opioids: the most addictive drugs in the world. Retrieved from https://www.vice.com/en/article/9bdymy/hamiltons-pharmacopeia-804-v16n4

Pottie, E., Tosh, D.K., Gao, Z.-G., Jacobson, K.A., and Stove, C.P. (2020a). Assessment of biased agonism at the A3 adenosine receptor using β-arrestin and miniGαi recruitment assays. Biochemical Pharmacology *177*, 113934.

Pottie, E., Dedecker, P., and Stove, C.P. (2020b). Identification of psychedelic new psychoactive substances (NPS) showing biased agonism at the 5-HT2AR through simultaneous use of β-arrestin 2 and miniGαq bioassays. Biochemical Pharmacology 114251.

Rajagopal, S., Ahn, S., Rominger, D.H., Gowen-MacDonald, W., Lam, C.M., DeWire, S.M., Violin, J.D., and Lefkowitz, R.J. (2011). Quantifying Ligand Bias at Seven-Transmembrane Receptors. Molecular Pharmacology *80*, 367–377.

Reavy, P. (2003). Utah case of potent drug is U.S. first. Retrieved from https://www.deseret.com/2003/6/3/19726293/utah-case-of-potent-drug-is-u-s-first

Renton, P., Green, B., Maddaford, S., Rakhit, S., and Andrews, J.S. (2012). NOpiates: Novel Dual Action Neuronal Nitric Oxide Synthase Inhibitors with μ-Opioid Agonist Activity. ACS Medicinal Chemistry Letters *3*, 227–231.

Rossi, A., Hunger, A., Kebrle, J., and Hoffmann, K. (1960a). Benzimidazol-Derivate und verwandte Heterocyclen IV. Die Kondensation von o-Phenylendiamin mit Alfa-Aryl- und Gamma-Aryl-acetessigester. Helvetica Chimica Acta *43*, 1046–1056.

Rossi, A., Hunger, A., Kebrle, J., and Hoffmann, K. (1960b). Benzimidazol-Derivate und verwandte Heterocyclen V. Die Kondensation von o-Phenylendiamin mit aliphatischen und alicyclischen Beta-Ketoestern. Helvetica Chimica Acta *43*, 1298–1313.

Shamai Yamin, T., Prihed, H., Shifrovitch, A., Dagan, S., and Weissberg, A. (2018). Oxidation-assisted

structural elucidation of compounds containing a tertiary amine side chain using liquid chromatography mass spectrometry. Journal of Mass Spectrometry *53*, 518–524.

Shulgin, A.T. (1975). Drugs of Abuse in the Future. Clinical Toxicology *8*, 405–456.

Siczek, M., Zawadzki, M., Siczek, M., Chłopaś-Konowałek, A., and Szpot, P. (2020). Etazene (N,N-diethyl-2-{[(4-ethoxyphenyl)methyl]-1H-benzimidazol-1-yl}-ethan-1-amine (dihydrochloride)): a novel benzimidazole opioid NPS identified in seized material: crystal structure and spectroscopic characterization. Forensic Toxicology.

Sorokin, V.I. (1999). Illegal synthesis of etonitazene. Journal of the Clandestine Laboratory Investigating Chemists Association *9*, 20.

Sorokin, V.I., Ponkratov, K.V., and Drozdov, M.A. (1999). Etonitazene encountered in Moscow. Microgram *32*, 239–244.

UNODC (2020a). World Drug Report 2020 (Austria: United Nations publication).

UNODC (2020b). The growing complexity of the opioid crisis. Global SMART Update, Volume 24 (Vienna).

Vandeputte, M.M., Cannaert, A., and Stove, C.P. (2020). In vitro functional characterization of a panel of non-fentanyl opioid new psychoactive substances. Archives of Toxicology *94(11)*, 3819–3830.

Vasudevan, L., Vandeputte, M.M., Deventer, M., Wouters, E., Cannaert, A., and Stove, C.P. (2020). Assessment of structure-activity relationships and biased agonism at the Mu opioid receptor of novel synthetic opioids using a novel, stable bio-assay platform. Biochemical Pharmacology 113910.

Verougstraete, N., Vandeputte, M.M., Lyphout, C., Cannaert, A., Hulpia, F., Van Calenbergh, S., Verstraete, A.G., and Stove, C.P. (2020). First report on brorphine: the next opioid on the deadly new psychoactive substances' horizon? Journal of Analytical Toxicology bkaa094.

Weissberg, A., Madmon, M., and Dagan, S. (2016). Structural identification of compounds containing tertiary amine side chains using ESI-MS3 combined with fragmentation pattern matching to chemical analogues – Benzimidazole derivatives as a case study. International Journal of Mass Spectrometry *394*, 9–21.

Wootten, D., Christopoulos, A., Marti-Solano, M., Babu, M.M., and Sexton, P.M. (2018). Mechanisms of signalling and biased agonism in G protein-coupled receptors. Nature Reviews Molecular Cell Biology *19*, 638–653.

Zagorski, C.M., Myslinski, J.M., and Hill, L.G. (2020). Isotonitazene as a contaminant of concern in the illegal opioid supply: A practical synthesis and cost perspective. International Journal of Drug Policy *86*, 102939.

Table 1. Summary of the analytical characterization.

	LC-QTOF-MS			GC-MS		HPLC-DAD	
	RTa (min)	**Parent (m/z)**	**Fragments (m/z)** **Bold: most abundant,** *italic: selective*	**RTa (min)**	**Fragments (m/z)**	**RTa (min)**	**Ab. max.[b] (nm)**
1. Isotonitazene	5.86	411.2436	44.05, 72.08, **100.11**, 107.05, 149.09, 250.11, 296.10	29.61	58, 86, 107	19.98	237.4 - 306.7
2. *N*-desethyl-isotonitazene	5.70	383.2095	44.05, **72.08**, 107.05, *176.05*, *224.09*, *270.08*, *312.13*	29.21	58, 107, 149, 325	20.13	238.4 - 305.8
3. 4'-OH-nitazene	3.94	369.1949	44.05, 72.08, **100.11**, 107.05, 250.11, 296.10	18.62*	58, 86, 107*	11.21	237.8 - 305.0
4. 5-aminoisotonitazene	3.42	381.2696	44.05, 72.08, **100.11**, 107.05, 149.09, *266.13*	26.89	58, 86, 107, 380	7.65	222.7 - 273.6 - 307.6
5. Metonitazene	4.91	383.2123	44.05, 72.08, **100.11**, 121.06, *264.13*, *310.12*	28.57	58, 86, 121	15.91	237.8 - 308.5
6. Etonitazene	5.44	397.2255	44.05, 72.08, **100.11**, 107.05, 135.08, *278.14*, *324.13*	29.58	58, 86, 107, 135	18.39	238.1 - 305.8
7. Protonitazene	6.11	411.2466	44.05, 72.08, **100.11**, 107.05, 149.10, 250.11, *292.16*, *338.15*	31.03	58, 86, 107	20.68	237.4 - 306.7
8. Clonitazene	5.57	387.1613	44.05, 72.08, **100.11**, *125.01*, *268.07*, *314.07*	28.09	58, 86, 125	18.63	238.4 - 305.8
9. Flunitazene	4.99	371.1890	44.05, 72.08, **100.11**, *109.04*, *252.11*, *298.10*	25.45	58, 86, 109	15.92	238.8 - 304.1
10. Isotodesnitazene	4.94	366.2573	44.05, 72.08, **100.11**, 107.05, 149.09, *251.11*	23.57	58, 86, 107, 365	14.37	269.6 - 276.6
11. Metodesnitazene	3.77	338.2251	44.05, 72.08, **100.11**, 121.06, 250.11, *265.13*	22.94	58, 86, 121, 337	7.89	269.6 - 276.6
12. Etodesnitazene	4.43	352.2409	44.05, 72.08, **100.11**, 107.05, 135.08, *279.15*	23.41	58, 86, 107, 135, 351	11.62	269.6 - 276.6

a, *retention time*; ***b***, *absorption maximum*; *, *alternative GC-MS method was employed (cfr. Methods section).*

Table 2. Overview of the potency (EC_{50}) and efficacy (E_{max}, relative to hydromorphone) data of the studied compounds (*n*=5). 95% confidence intervals are shown between brackets.

	MOR-βarr2		MOR-mini-Gi	
	EC_{50} (nM)	**E_{max} (%)**	**EC_{50} (nM)**	**E_{max} (%)**
1. Isotonitazene	**1.63** (1.17-2.28)	**179** (171-187)	**3.72** (2.62-5.26)	**381** (363-399)
2. *N*-desethyl-isotonitazene	**0.614** (0.377-0.985)	**229** (214-243)	**1.16** (0.798-1.70)	**421** (399-444)
3. 4'-OH-nitazene	**176** (124-250)	**133** (125-143)	**486** (329-705)	**223** (210-236)
4. 5-aminoisotonitazene	**383** (263-554)	**188** (176-201)	**761** (505-1119)	**298** (275-322)
5. Metonitazene	**8.14** (5.12-12.8)	**184** (172-197)	**23.5** (17.7-31.4)	**340** (326-355)
6. Etonitazene	**0.661** (0.338-1.26)	**219** (199-238)	**1.71** (1.23-2.42)	**397** (378-417)
7. Protonitazene	**3.95** (2.78-5.60)	**174** (165-182)	**10.4** (7.29-14.7)	**365** (347-384)
8. Clonitazene	**140** (93.6-210)	**173** (160-187)	**338** (204-559)	**303** (282-326)
9. Flunitazene	**377** (295-481)	**192** (183-202)	**827** (618-1094)	**255** (239-271)
10. Isotodesnitazene	**34.8** (22.1-54.4)	**155** (144-166)	**142** (105-191)	**309** (292-327)
11. Metodesnitazene	**548** (365-811)	**149** (139-159)	**1693** (1223-2358)	**224** (209-241)
12. Etodesnitazene	**54.9** (36.1-82.0)	**158** (147-169)	**164** (119-229)	**276** (261-290)
Fentanyl	**14.4** (11.5-18.0)	**163** (157-169)	**34.6** (25.0-47.7)	**282** (268-298)

Morphine	**338** (239-478)	**117** (111-123)	**385** (247-593)	**121** (115-127)
Hydromorphone	***36.2*** *(27.9-47.0)*	***100*** *(95.9-104)*	***49.3*** *(29.2-80.4)*	***100*** *(92.3-108)*

Figure legends

Figure 1. Structures of morphine, fentanyl, and isotonitazene. Isotonitazene, the prototypical member of the benzimidazole opioids, is structurally unrelated to traditional opiates or fentanyl.

Figure 2. Generic structure of the twelve studied nitazenes. Full chemical structures are shown in **Supplementary Data S1**.

Figure 3. General scheme depicting the synthesis of the different nitazenes included in this study **(1-12)** (Carroll and Coleman, 1975; Renton et al., 2012). Reagents and conditions: **(i)** *N*,*N*-diethylethylenediamine, EtOH, reflux; **(ii)** $(NH_4)_2S$, EtOH, reflux; **(iii)** *N*-ethoxycarbonyl-2-ethoxy-1,2-dihydroquinoline, CH_2Cl_2; **(iv)** HCl for **(7), (9)** and **(11)** or citric acid for **(10)** and **(12)**.

Figure 4. Graphical representation of the different fragments found by QTOF-MS. Different styles of arrows were used to allow easy identification of fragmentations that result in a given fragment.

Figure 5. Activation profiles (*n*=5) obtained for isotonitazene and **(A)** fentanyl, morphine and hydromorphone; **(B)** the metabolites *N*-desethyl-isotonitazene, 4'-OH-nitazene and 5-aminoisotonitazene; **(C)** metonitazene, etonitazene and protonitazene; **(D)** clonitazene and flunitazene; and **(E)** the desnitro-nitazenes isotodesnitazene, metodesnitazene, etodesnitazene. The left and right panels present data from the μ-opioid receptor (MOR) β-arrestin 2 and mini-Gi recruitment assays, respectively. Data are presented as mean receptor activation ± standard error of the mean (SEM) and are normalized to the maximum response of hydromorphone. Sixteen outliers (0.77%), as identified by the Grubbs' test, were excluded from the data set.

Figure 6. Quantitative μ-opioid receptor bias plot. Bias factors (β) ± SEM are plotted for all tested compounds, calculated from five independent experiments (*n*=5). Hydromorphone was used as unbiased reference agonist (β=0, not shown). Positive or negative bias factors imply a preference towards βarr2 or mini-Gi recruitment, respectively. None of the evaluated compounds showed statistically significant biased agonism at MOR, as compared to hydromorphone.